ChemComm

COMMUNICATION

View Article Online
View Journal | View Issue

Open Access Article. Published on 21 November 2016. Downloaded on 12/4/2025 9:09:24 PM.
This article is licensed under a Creative Commons Attribution 3.0 Unported Licence.

Cite this: *Chem. Commun.*, 2016, **52**, 14376

Received 8th September 2016,
Accepted 21st November 2016

DOI: 10.1039/c6cc07329h

www.rsc.org/chemcomm

High MOF loading in mixed-matrix membranes utilizing styrene/butadiene copolymers†

Jessica C. Moreton, Michael S. Denny, Jr. and Seth M. Cohen*

A series of styrene/butadiene polymers were combined with up to 90 wt% UiO-66 to form mixed-matrix membranes with varying physical properties. Notably, polystyrene-*block*-polybutadiene (SBS) membranes retained much of the processability and flexibility of the native polymer component and the porosity, chemical tunability, and adsorption of the native MOF.

Metal–organic frameworks (MOFs) are a class of crystalline materials with a wide range of tuneable properties. MOFs have been explored for a wide range of applications,[1] but the separation of gases or liquids by MOFs is an especially promising area because MOF pore size and functionality lend themselves well to selective discrimination between feed components.[2] These studies have led to interest in new, useful form factors for MOFs.[3]

Beyond microcrystalline solids, polycrystalline MOF membranes[4] have been prepared and demonstrate excellent separation performance, but suffer from difficult syntheses and limited MOF scope.[4] The mixed-matrix membrane form is an alternate approach towards MOF membranes that utilizes MOFs as the inorganic 'filler' component in polymer membranes.[5] MOFs can augment intrinsically porous polymer materials, with small amounts (generally <30 wt%)[6] of MOF doping sufficient to improve membrane properties such as flux[6e] for a variety of separation applications.[6c–e]

In addition to this MOF-doping approach, MMMs provide the opportunity to engineer MOF powders into a more useful, durable form factor through immobilization in a polymer. This route maximizes the MOF content in the MMM to create a membrane with chemical properties largely derived from the MOF, with the polymer primarily serving as a binder. In this approach, a MMM ideally attains properties like those of a polycrystalline MOF membrane, but with the added benefits of processability and robustness of the polymer (Fig. 1). Work by Ordoñez *et al.*[7] has shown the promise of high-MOF-content MMMs, where MMMs with >50 wt% of ZIF-8 in Matrimid® demonstrate improved selectivity for the separation of several different gas pairs, attributable to a shift from a "*polymer-driven to ZIF-8 controlled gas transport process*."[7] The increase in performance as this shift occurs demonstrates the value of a majority-MOF MMM approach.

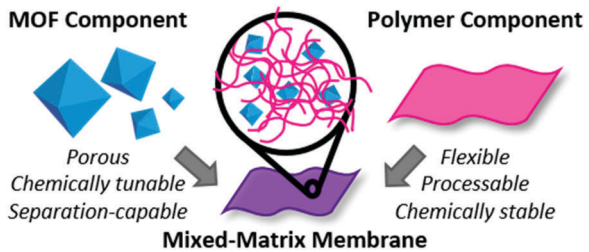

Fig. 1 MOF and polymer components combine to create a mixed-matrix membrane (MMM) with properties attributable to each material.

Another recent report described MOF-based MMMs that preserved the porosity, chemical tunability, and separation ability of the MOF, but in the form of a stable, flexible, freestanding membrane, essentially changing only the form factor of the MOF.[8] Using $\sim$70 wt% of various MOFs, MMMs were prepared with the fluoropolymer poly(vinylidene fluoride) (PVDF), a polymer with limited inherent porosity.[9] PVDF is among the only polymers identified to date that allow for high wt% MOF loadings and good adhesion to MOF particles.[10] However, PVDF is a specialized and expensive niche polymer, used primarily as a binder material in lithium-ion batteries.[11] Finding polymers other than PVDF that can make stable, high wt% MOF MMMs is an important goal, with few other options currently available. As such, we sought other polymers with different mechanical, chemical, and physical properties that could act as effective binders for MMMs with a high wt% of MOF.

Three polymer binders were explored in this study: pure polystyrene (abbreviated **PS**, $M_w = 35\,000$ g mol^{-1}), a polystyrene

Department of Chemistry and Biochemistry, University of California, San Diego, La Jolla, California 92093-0358, USA. E-mail: scohen@ucsd.edu

† Electronic supplementary information (ESI) available: Experimental procedures, PXRD, SEM, BET, mechanical testing, PSE, PSM, and dye filtration. See DOI: 10.1039/c6cc07329h

This journal is © The Royal Society of Chemistry 2016

Open Access Article. Published on 21 November 2016. Downloaded on 12/4/2025 9:09:24 PM.
This article is licensed under a Creative Commons Attribution 3.0 Unported Licence.

and polybutadiene block copolymer (**SBS**, M_w = 97 000 g mol^{-1}), and a random copolymer of styrene and butadiene (**SBR**, M_w = 270 000 g mol^{-1}). The polymers chosen for this study are commercially available (Sigma Aldrich) and have well established processing conditions and broad industrial uses.[12] **PS** is melted,[13] extruded,[14] and foamed,[15] providing a plethora of form factors for a mixed MOF/polymer system. Styrene/butadiene copolymers are broadly used[16] binder-type elastomers[11a] that could offer flexibility to a MMM. MOF-free films of pure **PS**, **SBS**, and **SBR** were readily formed by casting a polymer solution onto a substrate and removing the solvent by evaporation. These films displayed varying physical properties from highly brittle (**PS**) to tacky and stretchable (**SBR**), suggesting a range of final MMM physical properties. Given the few examples of polystyrene/MOF MMMs in the literature[17] a thorough investigation of these polymers in combination with MOFs was undertaken.

The Zr(IV)-based UiO-66[18] was used as a model MOF for forming MMMs. UiO-66 in this study consisted of uniform ~200 nm truncated, rounded octahedra, as confirmed by scanning electron microscopy (SEM, Fig. S1, ESI†). The bulk crystallinity of the MOF was confirmed by powder X-ray diffraction (PXRD, Fig. S2, ESI†) and porosity was assessed by N_2 sorption giving a BET surface area[19] of 1214 ± 44 m^2 g^{-1} (Fig. S3, ESI†).

MMMs were fabricated from a MOF-based viscous 'ink' of the MOF and polymer components in solution (Fig. S4, ESI†). The ink was prepared by first pre-dispersing the MOF and polymer components separately, then combining them to a homogeneous mixture of honey-like viscosity.[8] The MOF was dispersed by ultrasonication in a 1:1 mixture of THF and ethyl acetate (200 mg MOF per mL solvent) for roughly 30 min. The polymers were each dissolved in THF prior to combination with MOF. **PS** was dissolved to a concentration of 220 mg mL^{-1}, while **SBS** and **SBR** were dissolved to 100 and 50 mg mL^{-1}, respectively, yielding solutions of similar viscosity. These separate MOF and polymer solutions were then combined to yield final MOF wt% contents from 30% to 70% in each of the polymers tested, and ultrasonicated to homogeneity. The resulting ink was cast by the draw-down coating method. The MOF ink was transferred to an aluminium foil substrate, then cast with an automatic thick film coater (MTI Corp. MSK-AFA-II) using an adjustable doctor blade (blade height = 500 μm, speed = 25 mm per second), followed by drying (55 °C oven, 15 min) and delamination upon cooling, to yield membranes with thickness ranging from 50–100 μm.

All MMMs showed excellent retention of the MOF crystallinity as assessed by PXRD (Fig. S5–S8, ESI†). The polymers themselves were amorphous and did not contribute significantly to the PXRD pattern (Fig. S5, ESI†). Cross-section images obtained by SEM show retention of the MOF particle morphology within the membranes as well, further confirming that no significant changes to the structure of the MOF occurred upon incorporation into the MMM (Fig. 2 and Fig. S9–S18, ESI†).

At MOF loadings <70 wt%, SEM images of MMMs using all three polymers show dense films, with a large polymer presence and interspersed MOF (Fig. 2a, c and e). At MOF loadings ≥70 wt%, SEM cross-sections show a marked difference in morphology: very little polymer is seen in the SEM images, and

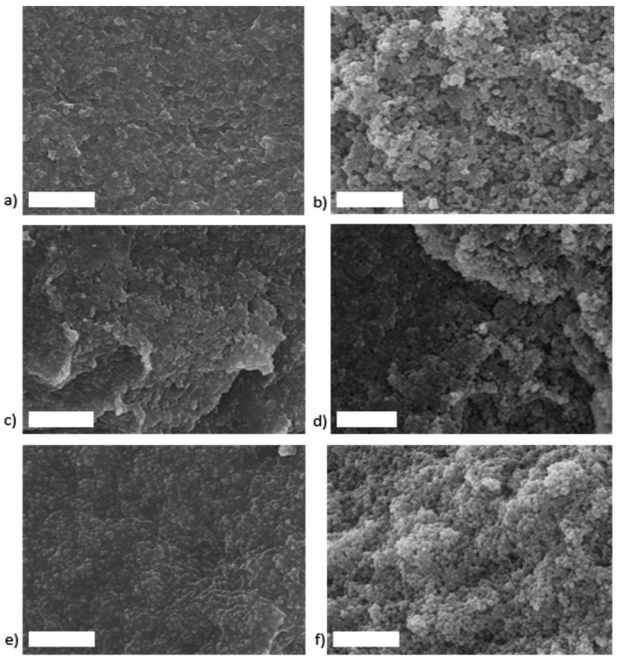

Fig. 2 SEM images of MMM cross-sections at 50 wt% (a, c and e) and 70 wt% (b, d and f) UiO-66 in polymers **PS** (a and b), **SBS** (c and d), and **SBR** (e and f). Scale bars are 5 μm.

membranes appear much more loosely packed (Fig. 2b, d and f). At 70 wt% MOF loadings in **SBS**, both morphologies are seen in a single membrane, highlighted in false-color SEM images (Fig. 4).

In contrast to earlier studies with PVDF-derived MMMs, N_2 sorption analysis revealed MMMs containing <70 wt% MOF to be non-porous (Table S1, ESI†). At ≥70 wt%, the surface area of the MOF was partially recovered (Fig. 3 and Table S1, ESI†) and type I isotherms were observed, which is characteristic of native UiO-66.[19] BET surface areas were calculated using the criteria proposed by Rouquerol[20] and explored by Snurr[21] for UiO-66 (see ESI†). The calculated surface areas of 70, 80, and 90 wt% UiO-66/**SBS** membranes were 578 ± 182 m^2 g^{-1}, 774 ± 32 m^2 g^{-1},

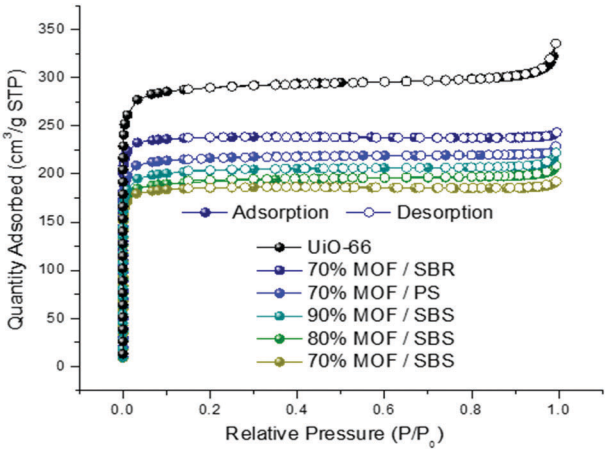

Fig. 3 N_2 sorption isotherms of all MMMs ≥ 70 wt% show the same characteristic microporosity as the native MOF. Adsorption and desorption branches are shown with filled and empty symbols, respectively.

Open Access Article. Published on 21 November 2016. Downloaded on 12/4/2025 9:09:24 PM.
This article is licensed under a Creative Commons Attribution 3.0 Unported Licence.

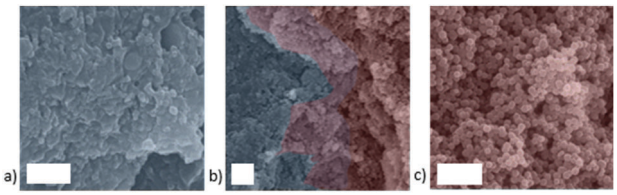

Fig. 4 False color SEM images of UiO-66/**SBS** MMMs at: (a) 50 wt%, (b) 70 wt%, and (c) 90 wt%. Dense (blue) and loose (red) membrane morphologies are highlighted. Scale bars are 2 μm.

and 781 ± 48 $m^2 g^{-1}$, respectively. Surface areas of 70 wt% UiO-66 in **SBR** and **PS** were 737 ± 248 $m^2 g^{-1}$ and 779 ± 114 $m^2 g^{-1}$, respectively, compared to the native UiO-66 surface area of 1214 ± 44 $m^2 g^{-1}$. Representative Rouquerol plots and BET constants are provided in the ESI† (Fig. S19 and Table S2). Pore size distributions demonstrate the preservation of the ~8.5 Å pores of UiO-66 (Fig. S20, ESI†).[22]

It is likely that the differences in surface area between the ≥70 wt% and <70 wt% formulations is a result of their different membrane morphologies. The total lack of surface area seen in membranes with MOF loading <70% corresponds to the dense morphology seen in these membranes (Fig. 2a, c, e, 4a and Fig. S9–S18, ESI†). Conversely, surface area is recovered in films with ≥70 wt% MOF that shows the more loosely packed particulate morphology (Fig. 2b, d, f, 4c and Fig. S9–S18, ESI†). Because the pure polymers show no inherent porosity, it is likely that when MOF particles are isolated in a higher quantity of impermeable polymer, the MOF pores are sealed and porosity is lost. Once the polymer content is sufficiently lowered, some MOF pores are again accessible, leading to partial recovery of surface area within the physically robust membrane.

Physically and mechanically, the MMMs resembled their pure-polymer counterparts. At the thicknesses studied (roughly 50–100 μm), **PS** MMMs were extremely brittle, and cracked upon delamination at all wt% MOF loadings, preventing analysis of bulk mechanical properties (Fig. S21, ESI†). **SBR** MMMs were extremely plastic and deformed readily upon delamination, which similarly hindered mechanical strength analysis; only films with high MOF loadings (70%) in **SBR** kept their shape upon physical manipulation sufficient to warrant testing (Fig. S22, ESI†). **SBS** MMMs delaminated easily and handled well at MOF contents from 30–90 wt% (Fig. S23, ESI†). Mechanical testing on **SBS** MMMs revealed MMMs up to 80 wt% MOF maintain higher tensile strength than both the pure polymer and the 70 wt% UiO-66/**SBR** MMM, quantitatively confirming the superior physical properties of the **SBS**-based MMMs tested (Fig. S24, S25 and Table S3, ESI†).

The preferable physical characteristics of **SBS** composites, coupled with their retention of porosity at high MOF loadings, warranted further studies to assess the chemical reactivity and accessibility of the MOF within the **SBS** membranes. The chemical reactivity of **SBS** MMMs were assessed by postsynthetic modification (PSM)[23] and exchange (PSE)[24] reactions. **SBS** MMMs fabricated with 80 wt% UiO-66-NH_2[23] were immersed in neat acetic anhydride for 24 h at 60 °C, washed with copious amounts of methanol, and analysed by ^{1}H NMR by digesting the MOF out of the MMM with hydrofluoric acid (HF). Essentially quantitative conversion of UiO-66-NH_2 to UiO-66-AM1[23] was observed (Fig. S26, ESI†), which is identical to that achieved with the native MOF. PSE experiments were carried out with 80 wt%-UiO-66/**SBS** MMMs immersed in solutions of 2-aminoterephthalate at 60 °C for 24 h, followed by copious washing with both water and methanol. PSE was also successful, achieving ~17% exchange of terephthalic acid for the amine-functionalized linker (Fig. S27, ESI†) compared to 45% exchange in the native UiO-66 control.

MMMs subjected to PSM and PSE reactions were assessed for their post-reaction mechanical integrity and preservation of MOF quality. Post-PSM MMMs fractured in the reaction solution, confirming lower mechanical stability compared to the unmodified 80 wt% MMM. MMMs after PSE survived the reaction conditions intact, but upon quantitative mechanical analysis, lost strength and elasticity relative to both the starting 80 wt% MMM and the pure polymer (Fig. S28, S29 and Table S3, ESI†). However, after PSM or PSE the MOFs in these MMMs retained their crystallinity, porosity, and morphology, as assessed by PXRD, N_2 gas sorption and SEM, respectively (Fig. S30–S32 and Table S4, ESI†).

Dye filtration studies were used to further demonstrate the accessibility of the MOF pores in the **SBS** MMMs. Previous studies document the ability of UiO-66 to adsorb charged dye molecules from aqueous solutions.[8,25] 80 wt% UiO-66/**SBS** MMMs were housed in 13 mm Swinnex® syringe filters, and 10 μM dye solutions were passed through the membranes in a dead-stop filtration set-up. Coomassie Brilliant Blue R-250 was retained with 60% fidelity (Fig. S33, ESI†), but consistent with previous studies,[8] anionic Methyl Orange was not retained in the membrane, achieving only 22% retention (Fig. S34, ESI†). MMMs used for Coomassie blue filtration also showed good recyclability (Fig. S35, ESI†). The retention of the dye adsorption ability of UiO-66 within the MMM form factor over multiple cycles demonstrates that the MOF pore chemistry and functionality is retained, and its processability is certainly markedly increased in the membrane form factor.

In summary, new MOF MMMs have been successfully fabricated that add the physical flexibility and strength of the polymer to the existing chemical abilities of the MOF. Retention of porosity was seen in high MOF loadings in MMMs of all three polymers, and the mechanical superiority of **SBS** made it the most viable formulation. Postsynthetic chemical reactions and dye filtration experiments on the sturdy **SBS** membranes demonstrate the chemical accessibility of the MOF, confirming that all major MOF characteristics are preserved within the **SBS** MMMs. In comparison with previously studied PVDF, **SBS** offers similar levels of durability and chemical inertness at lower cost and with wider availability. The **SBS** MMMs fabricated also achieve higher MOF loadings than PVDF, maximizing the active component of the MMM to unprecedented levels for this approach. This form factor can promote the direct application of MOF materials to a myriad of membrane-based technologies, such as catalytic reactors,[26] commercial separations of gas streams,[27] wastewater treatment,[28] toxic chemical sequestration,[29] and more. Moving forward, the block copolymer nature of **SBS** lends it to

Open Access Article. Published on 21 November 2016. Downloaded on 12/4/2025 9:09:24 PM.
This article is licensed under a Creative Commons Attribution 3.0 Unported Licence.

greater mechanical tunability than PVDF, through variation of the relative amounts of styrene and butadiene. The favourable physical and chemical properties, low cost, and wide availability of **SBS** make it an attractive binder for MOF-based MMMs.

This work was financially initiated by the Army Research Office (STIR-W911NF-15-1-0497), with continuing support from the National Science Foundation (DMR-1506059). The authors acknowledge Michael Frank and Prof. Joanna McKittrick (Dept. of Mechanical and Aerospace Engineering, UCSD) for assistance with mechanical testing.

Notes and references

1 (*a*) H. Furukawa, K. E. Cordova, M. O'Keeffe and O. M. Yaghi, *Science*, 2013, **341**, 1230444; (*b*) P. Horcajada, R. Gref, T. Baati, P. K. Allan, G. Maurin, P. Couvreur, G. Férey, R. E. Morris and C. Serre, *Chem. Rev.*, 2012, **112**, 1232–1268; (*c*) J. Lee, O. K. Farha, J. Roberts, K. A. Scheidt, S. T. Nguyen and J. T. Hupp, *Chem. Soc. Rev.*, 2009, **38**, 1450–1459.
2 (*a*) E. Adatoz, A. K. Avci and S. Keskin, *Sep. Purif. Technol.*, 2015, **152**, 207–237; (*b*) B. Li, H.-M. Wen, W. Zhou and B. Chen, *J. Phys. Chem. Lett.*, 2014, **5**, 3468–3479.
3 (*a*) M. S. Denny, Jr., J. C. Moreton, L. Benz and S. M. Cohen, *Nat. Rev. Mater.*, 2016, **1**, DOI: 10.1038/natrevmats.2016.78; (*b*) B. Böhringer, R. Fischer, M. R. Lohe, M. Rose, S. Kaskel and P. Küsgens, in *Metal–Organic Frameworks*, ed. D. Farrusseng, Wiley-VCH Verlag GmbH & Co. KGaA, Weinheim, Germany, 2011, pp. 353–381.
4 A. Bétard and R. A. Fischer, *Chem. Rev.*, 2012, **112**, 1055–1083.
5 B. Zornoza, C. Tellez, J. Coronas, J. Gascon and F. Kapteijn, *Microporous Mesoporous Mater.*, 2013, **166**, 67–78.
6 (*a*) M. Amirilargani and B. Sadatnia, *J. Membr. Sci.*, 2014, **469**, 1–10; (*b*) J. E. Bachman, Z. P. Smith, T. Li, T. Xu and J. R. Long, *Nat. Mater.*, 2016, **15**, 845–849; (*c*) S. Basu, M. Maes, A. Cano-Odena, L. Alaerts, D. E. De Vos and I. F. J. Vankelecom, *J. Membr. Sci.*, 2009, **344**, 190–198; (*d*) J. Duan, Y. Pan, F. Pacheco, E. Litwiller, Z. Lai and I. Pinnau, *J. Membr. Sci.*, 2015, **476**, 303–310; (*e*) W. Li, Y. Zhang, Q. Li and G. Zhang, *Chem. Eng. Sci.*, 2015, **135**, 232–257.
7 M. J. C. Ordoñez, K. J. Balkus Jr, J. P. Ferraris and I. H. Musselman, *J. Membr. Sci.*, 2010, **361**, 28–37.
8 M. S. Denny and S. M. Cohen, *Angew. Chem., Int. Ed.*, 2015, **54**, 9029–9032.
9 Y. Shen and A. C. Lua, *Chem. Eng. J.*, 2012, **192**, 201–210.
10 (*a*) J. B. DeCoste, J. M. S. Denny, G. W. Peterson, J. J. Mahle and S. M. Cohen, *Chem. Sci.*, 2016, **7**, 2711–2716; (*b*) Y. Han, P. Qi, J. Zhou, X. Feng, S. Li, X. Fu, J. Zhao, D. Yu and B. Wang, *ACS Appl. Mater. Interfaces*, 2015, **7**, 26608–26613.
11 (*a*) H. Buqa, M. Holzapfel, F. Krumeich, C. Veit and P. Novák, *J. Power Sources*, 2006, **161**, 617–622; (*b*) X. Zhang, P. N. Ross, R. Kostecki, F. Kong, S. Sloop, J. B. Kerr, K. Striebel, E. J. Cairns and F. McLarnon, *J. Electrochem. Soc.*, 2001, **148**, A463–A470.
12 M. Mihai, M. A. Huneault and B. D. Favis, *J. Cell. Plast.*, 2007, **43**, 215–236.
13 G. Welsh, in *Modern Styrenic Polymers: Polystyrenes and Styrenic Copolymers*, ed. J. Scheirs and D. B. Priddy, John Wiley & Sons, Chichester, UK, 2003, pp. 233–246.
14 N. Niessner and H. Gausepohl, in *Modern Styrenic Polymers: Polystyrenes and Styrenic Copolymers*, ed. J. Scheirs and D. B. Priddy, John Wiley & Sons, Chichester, UK, 2003, pp. 25–42.
15 K. Suh and A. Paquet, in *Modern Styrenic Polymers: Polystyrenes and Styrenic Copolymers*, ed. J. Scheirs and D. B. Priddy, John Wiley & Sons, Chichester, UK, 2003, pp. 203–231.
16 R. R. Lattime, *Styrene-Butadiene Rubber*, Kirk-Othmer Encyclopedia of Chemical Technology, 2000.
17 (*a*) J. T. Culp, L. Sui, A. Goodman and D. Luebke, *J. Colloid Interface Sci.*, 2013, **393**, 278–285; (*b*) M. Rose, B. Böhringer, M. Jolly, R. Fischer and S. Kaskel, *Adv. Eng. Mater.*, 2011, **13**, 356–360; (*c*) W. S. Chi, S. Hwang, S.-J. Lee, S. Park, Y.-S. Bae, D. Y. Ryu, J. H. Kim and J. Kim, *J. Membr. Sci.*, 2015, **495**, 479–488.
18 J. H. Cavka, S. Jakobsen, U. Olsbye, N. Guillou, C. Lamberti, S. Bordiga and K. P. Lillerud, *J. Am. Chem. Soc.*, 2008, **130**, 13850–13851.
19 H. Wu, Y. S. Chua, V. Krungleviciute, M. Tyagi, P. Chen, T. Yildirim and W. Zhou, *J. Am. Chem. Soc.*, 2013, **135**, 10525–10532.
20 J. Rouquerol, P. Llewellyn and F. Rouquerol, in *Studies in Surface Science and Catalysis*, ed. P. L. Llewellyn, F. Rodriquez-Reinoso, J. Rouqerol and N. Seaton, Elsevier, 2007, vol. 160, pp. 49–56.
21 (*a*) D. A. Gómez-Gualdrón, P. Z. Moghadam, J. T. Hupp, O. K. Farha and R. Q. Snurr, *J. Am. Chem. Soc.*, 2016, **138**, 215–224; (*b*) K. S. Walton and R. Q. Snurr, *J. Am. Chem. Soc.*, 2007, **129**, 8552–8556.
22 M. J. Katz, Z. J. Brown, Y. J. Colon, P. W. Siu, K. A. Scheidt, R. Q. Snurr, J. T. Hupp and O. K. Farha, *Chem. Commun.*, 2013, **49**, 9449–9451.
23 S. J. Garibay and S. M. Cohen, *Chem. Commun.*, 2010, **46**, 7700–7702.
24 M. Kim, J. F. Cahill, Y. Su, K. A. Prather and S. M. Cohen, *Chem. Sci.*, 2012, **3**, 126–130.
25 B.-J. Yao, W.-L. Jiang, Y. Dong, Z.-X. Liu and Y.-B. Dong, *Chem. – Eur. J.*, 2016, **22**, 10565–10571.
26 I. F. J. Vankelecom, *Chem. Rev.*, 2002, **102**, 3779–3810.
27 B. Seoane, J. Coronas, I. Gascon, M. E. Benavides, O. Karvan, J. Caro, F. Kapteijn and J. Gascon, *Chem. Soc. Rev.*, 2015, **44**, 2421–2454.
28 D. Qadir, H. Mukhtar and L. K. Keong, *Sep. Purif. Rev.*, 2017, **46**, 62–80.
29 J. B. DeCoste and G. W. Peterson, *Chem. Rev.*, 2014, **114**, 5695–5727.